J. Fluid Mech. (1980), *vol.* 96, *part* 2, *pp.* 223–241
Printed in Great Britain

Multipole expansion calculation of slow viscous flow about spheroids of different sizes

By WEI-HSI LIAO AND DAVID A. KRUEGER
Department of Physics, Colorado State University, Fort Collins, Colorado 80523

(Received 17 April 1978 and in revised form 15 January 1979)

The multipole representation technique of Gluckman, Pfeffer & Weinbaum for slow, viscous, axisymmetric motion has been applied to a system of two spheroids. The two particles may have different shapes and volumes. The limitations of this method have been studied through calculations of the drag forces and velocities of particles with aspect ratios from 0·1 to 10 and relative volumes V from 1 to 10^3. The multipole-expansion convergence is quite slow for large relative volumes and requires on the order of $4 \times V^{\frac{1}{3}}$ multipoles. Wild fluctuations in the drag as the number of multipoles increases were found for large oblate spheroids. Relative velocities are given quite accurately for separations of the centres greater than 1·02 times the minimum separation. Comparisons are made with previous results and approximate theories for two spheres, for non-identical particles at large separation, and for a sphere near a large spheroid.

1. Introduction

Recent experimental observations indicate that large agglomerates form when some magnetic colloids are exposed to uniform magnetic fields (Peterson *et al.* 1975; Peterson 1975; Peterson & Krueger 1977). The experiments were interpreted in terms of the gravitational settling of agglomerates consisting of roughly 10^8 colloidal particles. The size of the agglomerates was deduced from observations of the terminal velocity and was found to depend significantly upon the applied magnetic field. If one assumes that the hydrodynamic drag force overcomes the magnetic force and is responsible for pulling particles off the agglomerate as it falls, one can calculate the agglomerate size as a function of applied magnetic field (Liao & Krueger 1979). To do this, one needs to know the drag forces on two spheroids of different sizes and shapes. The drag force on pairs of unlike, non-spherical particles is also applicable in problems of agglomeration of aerosol particles and removal of particulates from flows. A closely related problem is to determine the motion of pairs or groups of particles in an external force field such as gravity.

The slow viscous motion of particles in a fluid has a long history including the classic work of Stokes on the drag force on a single sphere,† see, e.g., Lamb (1932). The drag on single ellipsoids can also be found in Lamb. The two-particle problem is less tractable, but Stimson & Jeffery (1926) presented the solution for the drag on two unequal spheres moving with the same velocity in terms of an infinite sum. Cooley & O'Neill (1969) gave numerical values for these forces for spheres of different sizes

† Oseen corrections are ignored.

0022-1120/80/4345-7870 $02.00

moving along their line of centres at various separations. Wacholder & Sather (1974) calculated the velocities of pairs of unequal spheres moving in a fluid under gravity. These calculations on pairs of spheres are not generalizable to other particle shapes or to more than two spheres because they depend upon the existence of an exact solution in bispherical co-ordinates. A more general formulation introduced by Youngren & Acrivos (1975*a*) is in terms of a linear integral equation for the distribution of Stokeslets over the particle surfaces. They have used this technique to calculate the rotational frictional coefficients for ellipsoids and a benzene-like shape (1975*b*) and to calculate the shape of a gas bubble in a viscous flow (1976). For computation the integral equation is reduced to solving a set of linear algebraic equations for the surface-stress force, $\mathbf{f}(\mathbf{x})$, for a given geometry and velocity of the fluid on the surface of the particles (see equation (2.9) of Youngren & Acrivos, 1975*a*). They point out that one of the main advantages of this technique is that the matrix of the algebraic system need be inverted only once. However, the matrix *must* be inverted for each change in the *geometry*. In addition the method is more complicated for two particles moving at different velocities under the influence of an external force such as gravity. In that case the velocities are not known *a priori* but must be calculated. If the total drag force on each particle is assumed to be balanced by the gravitational force, then the integral of $\mathbf{f}(\mathbf{x})$ over a surface is fixed but $\mathbf{f}(\mathbf{x})$ must be calculated. This could be accomplished by taking an appropriate linear combination of the $\mathbf{f}$'s calculated for two basic cases such as unit velocity on the first particle, zero velocity on the second particle and then vice versa. In view of these complications for our problem we have chosen to use the collocation technique.

A set of linear algebraic equations is also the result of a collocation approach introduced by O'Brien (1968) who expanded the stream function as a truncated series of separable solutions in spherical co-ordinates. Bowen & Masliyah (1973) generalized this by using a series of separable solutions in spheroidal co-ordinates for single closed bodies of revolution. Gluckman, Pfeffer & Weinbaum (1971) used a similar series representation of the stream function to calculate the drag on two or more identical spheroids aligned along the direction of fluid flow. In the collocation approach the stream function is approximated by a truncated series of multi-lobular disturbances. The accuracy of the representation is systematically improved by the addition of higher-order multipoles. The coefficients in this expansion are determined by satisfying the boundary conditions at a finite number of points, i.e. by solving a finite set of linear equations. The number of multipoles required for a given accuracy is not known in general. However, for two or more touching identical prolate spheroids, the error in the drag force was less than 2·5 % when only the first two multipoles for each particle were included. For an arbitrary convex axisymmetric particle Gluckman, Weinbaum & Pfeffer (1972) used the collocation technique with a superposition of oblate spheroid solutions. The collocation–multipole expansion technique has been used to investigate unsteady forces (Basset, virtual mass, and acceleration) for chains of identical spheres falling along the chain axis (Leichtberg, Weinbaum, Pfeffer & Gluckman 1976*c*). These results have been used to understand the rouleaux formation by red blood cells (Leichtberg, Weinbaum & Pfeffer 1976*b*) and to investigate the effects of walls (Leichtberg, Pfeffer & Weinbaum 1976*a*). Ganatos, Pfeffer & Weinbaum (1978) have also used this technique to study more general motions of identical spheres. Because of the success of this technique in those cases where identical particles were

considered, we have extended it to non-identical particles and have determined some of its limitations.

To study the limitations we first calculated the drag on two touching spheres of different radii. These cases were selected (*a*) because it is a severe test of the technique to handle the strong particle–particle interactions at contact and (*b*) because exact results are available for comparison. We have varied the number of multipoles and find that roughly $V^{\frac{1}{3}}$ multipoles are required, where V is the relative volume of the spheres. We have also varied the location of the points where the boundary conditions are to be satisfied and find that as V increases the results become more sensitive to the location. In the low Reynolds number limit, we have also calculated the velocity of axisymmetric gravitational settling of nonidentical spheroids as a function of their separation. From this one could calculate their motion as a function of time. A comparison with analytic asymptotic results gives the region of applicability of the asymptotic formulas as well as testing the collocation calculation.

We have introduced a renormalization procedure which minimizes a numerical difficulty encountered when including high multipoles. In addition we show how to calculate the required Gegenbauer functions using single-precision, real arithmetic on the computer in place of double-precision, complex arithmetic as has been done in the past for oblate spheroids.

In the next four sections we review the basic formalism, give results for drag forces, give results for settling velocities, and present our conclusions. Appendix A gives an analytic argument to estimate the number of multipoles required.

2. Formalism

Consider two spheroids moving along the x axis as shown in figure 1. In terms of the stream function, ψ, for the axially symmetric case the components of the fluid velocity along the x axis, U_x, and radially outward, U_r, are given by

$$U_x = \frac{1}{r}\frac{\partial \psi}{\partial r}, \quad U_r = -\frac{1}{r}\frac{\partial \psi}{\partial x}. \tag{2.1}$$

The no-slip boundary condition requires that the fluid velocity on the surface of a particle is the same as the velocity of that particle. The fluid velocity goes to zero as $\rho = (x^2+r^2)^{\frac{1}{2}}$ goes to infinity. For two spheroids designated by S and L, we take a general solution as

$$\psi = \psi^S + \psi^L. \tag{2.2}$$

For spherical co-ordinates, ψ^S is of the form

$$\sum_{n=2}^{\infty} [D_{n,S} r^{-n+3} + B_{n,S} r^{-n+1}] I_n(\theta). \tag{2.3}$$

For prolate or oblate spheroidal co-ordinates, the function ψ^S is of the form (Gluckman *et al.* 1971; Happel & Brenner 1973)

$$[D_{2,S} p_S + B_{2,S} H_2(p_S) + D_{4,S} H_4(p_S)] I_2(q_S) + [D_{3,S} + B_{3,S} H_3(p_S) + D_{5,S} H_5(p_S)] I_3(q_S) + \sum_{n=4}^{\infty} (D_{n,S} H_{n-2}(p_S) + B_{n,S} H_n(p_S) + D_{n+2,S} H_{n+2}(p_S)] I_n(q_S). \tag{2.4}$$

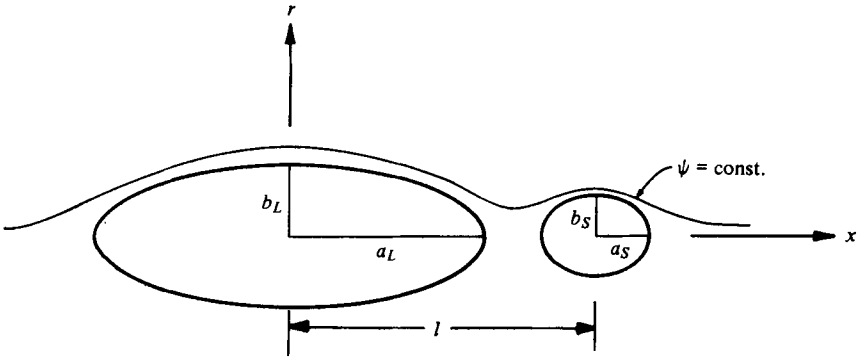

FIGURE 1. Axisymmetric motion of two spheroids.

The function ψ^L is given by a similar expression. Here $I_n(q)$ and $H_n(p)$ are Gegenbauer functions of the first and second kind respectively and are linear combinations of the Legendre functions of the first and second kind (P_n and Q_n). For each particle the p and q values are relative to a co-ordinate system with an origin at the centre of that particle. The x axis is always the symmetry axis and the particle intersects the x axis at a and the y axis at b. For a prolate particle, $a > b > 0$, $c^2 = a^2 - b^2$, $x = c\cosh\xi\cos\eta$, $r = c\sinh\xi\sin\eta$ and $p = \cosh\xi$. For an oblate particle, $b > a > 0$, $c^2 = b^2 - a^2$, $x = c\sinh\xi\cos\eta$, $r = c\cosh\xi\sin\eta$, $p = i\sinh\xi$ and $i = \sqrt{-1}$. In both cases $q = \cos\eta$, $\xi_0 \leqslant \xi \leqslant \infty$, and $0 \leqslant \eta \leqslant \pi$.

We first consider the drag force on the particles when the velocities are equal to U. Defining λ_j by the expression (where j is either S or L)

$$F_j \equiv 6\pi\mu U b_j \lambda_j \tag{2.5}$$

where μ is the fluid viscosity, Gluckman *et al.* (1971) give

$$\lambda_j = 2D_{2,j}/(3c_j b_j U). \tag{2.6}$$

This expression is also valid for spheres if one deletes the c_j factor.

Thus the total drag is completely determined by the first coefficient, D_2, in the expansion (2.4). However, D_2 can be found only by applying the boundary conditions which involve all the other D's and B's. The essential assumption of the truncation technique is that D_2, determined approximately by satisfying the boundary conditions through use of only a few multipoles (i.e. D's and B's), will not change appreciably as additional multipoles are included. For chains of identical particles, Gluckman *et al.* (1971) found that including only D_2, B_2, D_3 and B_3 terms gave results accurate to 2·5 %. The present work focuses on the convergence for two particles of different sizes and shapes.

Firstly ψ^S is truncated to include terms $D_{2,S}$, $B_{2,S}$ through $D_{m+1,S}$, $B_{m+1,S}$. Similarly ψ^L is truncated to include terms $D_{2,S}$, $B_{2,S}$ through $D_{n+1,L}$, $B_{n+1,L}$. This gives $2(n+m)$ D's and B's to be determined. These coefficients are determined by requiring that ψ satisfy the two boundary conditions (from the two components of the velocity) on N_S points on the S particle surface and N_L points on the L particle surface, where $N_S + N_L = n+m$. We have further taken $N_S = m$ and $N_L = n$.

This yields the matrix equation

$$\mathbf{MD} = \mathbf{R} \tag{2.7}$$

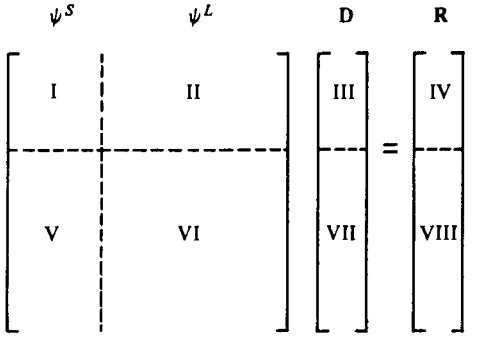

FIGURE 2. Schematic diagram of equation (2.7).

with **M** equal to an $N \times N$ matrix and **D** and **R** equal to vectors of length $N = 2(n+m)$. **D** is the vector of unknown coefficients $(D_{2,S}, B_{2,S}, \ldots, D_{2,L}, B_{2,L}, \ldots)$. The first $2m$ elements of **R** are proportional to the velocity of the S particle and the last $2n$ elements are proportional to the velocity of the L particle.†

The elements of **M** are given by Gegenbauer functions of the first and second kinds ($I_n(q)$, $H_n(p)$) and their derivatives. $H_n(p)$ and its derivative become extremely small for large p ($|p| = a/c$ on the surface of the particle) as well as large n. Thus including more multipoles increases the chance of ill-conditioning in the solution to (2.7). For example, for two touching, almost spherical particles with relative volume $V = 10^3$, and $n = m = 12$, there exists 73 orders of magnitude difference between the largest and smallest elements in the matrix **M**. Instead of going to an iteration matrix reduction scheme plus double-precision arithmetic as suggested by Gluckman *et al.* (1971), the ill-conditioning can be reduced dramatically with a renormalization. Equation (2.7) is shown schematically in figure 2, where I, II and IV have $(2m)$ rows obtained by satisfying boundary conditions on m points on the S particle surface and V, VI and VIII have $(2n)$ rows obtained by satisfying boundary conditions on n points on the L particle surface. The renormalization takes three steps. The first step is to make the elements in IV and VIII have the same order of magnitude. This is done by dividing elements in V, VI and VIII by a constant. The second step is to make the first elements in III ($D_{2,S}$) and VII ($D_{2,L}$) have the same magnitude. This is done by dividing elements in II and IV by a constant. Finally, the first row elements of I and VI are multiplied by constants to make them unity, while the elements of the **D** vector are divided by these same constants. In the example mentioned above this brings the elements of I, II and VI to within about four orders of magnitude. For the S particle being the smaller particle, the first column of V is of the same order as I, II, and VI but subsequent columns decrease rapidly. This is a result of higher multipoles of ψ^S becoming smaller as one moves away from the smaller particle.

Finally often it is convenient to calculate the Gegenbauer functions of the second kind and their derivatives [i.e. $H_n(p)$ and $H'_n(p)$] by using the recursion relation downward for $Q_n(p)$ [$H_n(p)$ and $H'_n(p)$ can be found from $Q_n(p)$] rather than upward as was done in some cases by Gluckman *et al.* To calculate $Q_n(p)$ to more than 15 place

† Note that since the velocities and D_2 appear linearly in (2.7) it follows that the magnitude of the drag is the same for the S particle following or leading the L particle.

accuracy for $0 \leqslant n \leqslant 50$ and $p \geqslant 1{\cdot}09$, one takes $Q_{90}(p) = 10^{-80}$ and $Q_{89}(p) = 10^{-80}$† and calculates $Q_{88}, \ldots, Q_0$ using the recursion relation. Finally one multiplies all the values obtained by the constant required to make Q_0 its known value (i.e. obtained from equation (2.12)).

For oblate spheroids p is purely imaginary. This led Gluckman *et al.* (1971) to use double-precision complex arithmetic to calculate $H_n(iy)$, where y is real. For computations we define $\bar{H}_n$ and $\bar{Q}_n$ by

$$H_{n+1}(p) = \delta_n \bar{H}_n(|p|), \tag{2.8a}$$

$$Q_{n-1}(p) = \delta_n \bar{Q}_n(|p|), \tag{2.8b}$$

where $\delta_n = +1$ for the prolate case. For the oblate case (p is imaginary) we have $\delta_n = 1$ for n even and $\delta_n = i$ for n odd. Note that $p \geqslant 1$ for the prolate case and $p/i \geqslant 0$ for the oblate case. The $\bar{H}_n$ and $\bar{Q}_n$ are real quantities. This leads to the recursion

$$(n+1)\,\bar{Q}_{n+2} = (2n+1)\,|p|\,\sigma^{n+1}\bar{Q}_{n+1} - n\bar{Q}_n, \tag{2.9}$$

where $\sigma = +1$ for p real (prolate) and $\sigma = -1$ for p imaginary (oblate). $\bar{H}_n$ and its derivative are obtained from the $\bar{Q}$'s as

$$(2n+1)\,\bar{H}_n = \bar{Q}_n - \bar{Q}_{n+2} \tag{2.10}$$

and

$$\partial \bar{H}_n/\partial p = -\delta_{n+1}\bar{Q}_n/\delta_n. \tag{2.11}$$

For p real and greater than 1, Gautschi (1967) has shown that using the recursion downward is stable. We have used it downward for $|p| \geqslant 1{\cdot}09$. For $|p| < 1{\cdot}09$ we have used the recursion upward, where

$$\bar{Q}_1 = \tfrac{1}{2}\ln((p+1)/(p-1)) \quad \text{prolate}, \tag{2.12a}$$

$$\bar{Q}_1 = \tan^{-1}(|p|) - \tfrac{1}{2}\pi \quad \text{oblate} \tag{2.12b}$$

and

$$\bar{Q}_2 = \sigma|p|\,\bar{Q}_1 - 1. \tag{2.13}$$

To this point we have discussed the calculation of the drag forces if the velocities of the particles are specified. Next we turn to the calculation of the velocities of the particles when a specified external force is acting (e.g. gravity). As discussed by Leichtberg *et al.* (1976*c*), to leading order in Reynolds number, the drag force $(4\pi\mu D_2/c)$ is balanced by the external force, which is $\frac{4}{3}\pi(\rho_0 - \rho)\,ab^2 g$ in the case of gravity. Here ρ_0 is the density of the solid, ρ is the density of the liquid, and g is the acceleration due to gravity (980 cm s^{-2}). This gives

$$D_2 = (\rho_0 - \rho)\,gcab^2/(3\mu). \tag{2.14}$$

This equation is valid for prolate and oblate spheroids. We can include spheres if we delete the c factor. Using this expression for both $D_{2,S}$ and $D_{2,L}$ in the **MD = R** equation results in linear equations which may be solved for $B_{2,S}\,D_{3,S}, \ldots, B_{2,L}$, $D_{3,L}, \ldots, U_S$ and U_L.

† 10^{-80} can be replaced by any small number. Then

$$10^{-80} = \alpha P_{90} + \beta Q_{90} \quad \text{and} \quad 10^{-80} = \alpha P_{89} + \beta Q_{89},$$

where P_n is the Legendre function of the first kind. Since $P_{89} \gg Q_{89}$ for large arguments these equations guarantee that α is very small and what we compute is basically βQ_n for $n \lesssim 50$.

3. Numerical results for drag forces

(*a*) We first consider two touching particles to illustrate some of the limitations of the method. In all calculations the motion is along the line of centres. Within the approximation of continuum fluid mechanics, it takes an infinite force to separate two particles in contact as has been discussed by Leichtberg *et al.* (1976*c*). Thus the two particles will move at the same speed. In this section we calculate the resulting dimensionless drag coefficient λ. We consider (1) the sensitivity to the location of the points where the boundary conditions are imposed for two spheres, (2) the optimum number of multipoles for two spheres, and (3) the drag on non-spherical particles.

As a check on the computer code we have calculated the drag on two identical particles. We have reproduced the results given by Gluckman *et al.* (1971) for combinations of aspect ratios ($\kappa = b/a = 1, 0{\cdot}5, 5{\cdot}0$), separation of centres ($d_0/a + 2 = 1, 4, 16$), and numbers of points $N_S = N_L = 6$, 8, 10, 12). Calculations for widely separated particles with $\kappa = 0{\cdot}1$, 1, and 10 and relative volumes of 1 and 10^3 were also checked. In addition we find consistent results for a small sphere touching a large nearly spherical particle (relative volume = 10^3) using $\kappa_L = 0{\cdot}99$, $1{\cdot}0$, or $1{\cdot}01$.

(*b*) To determine the optimum number and locations of the collocation points we consider two touching spheres because exact results are available for comparison. We have considered several sets of angles of the points where the boundary conditions are applied. Note $\eta = 0$ is the + symmetry axis, x, and $\eta = \frac{1}{2}\pi$ is along r in figure 1, and $\eta = \pi$ is the $-x$ axis. Unless otherwise noted we follow Gluckman *et al.* (1971) and take points as mirror image pairs about $\eta = \frac{1}{2}\pi$. For η odd, the mirror image of the smallest η point is omitted. The pair of points closest to $\eta = \frac{1}{2}\pi$ are chosen to be very close to the highest point on the generating arc to represent the projected area normal to the direction of the flows and at the same time to avoid the singularity problem at $\eta = \frac{1}{2}\pi = 90°$. We take points at 89° and 91°. If the number of points is greater than 2, we place points at η_α and $\pi - \eta_\alpha$. The interval between η_α and 89° is divided into equal intervals, η_β, for sets of angles A, B, and C. We take $\eta_\alpha = \eta_\beta$ for set A, $\eta_\alpha = 1°$ for set B, and $\eta_\alpha = 6°$ for set C. The set of points used by Gluckman *et al.* is denoted by G and is obtained by taking $\eta_\alpha = \eta_\beta = \pi/N$ and taking a point at 89°. Sets G and A differ only in that they take equal division of 90° and 89° respectively.

Table 1 gives the results for λ_S and λ_L for identical spheres in contact. The exact value given by Cooley & O'Neill (1969) is 0·645141. For $N_S = N_L$ we have entered $\lambda_S = \lambda_L$. For $N_S \neq N_L$ the upper number is λ_S and the lower number is λ_L. Of course λ_S should still equal λ_L. From table 1 the average of λ_S and λ_L is very nearly the exact value but for $N_L \neq N_S$ set A gives the best results for the values of λ_S and λ_L. Other calculations for touching spheres with relative volume of 10^4 and with $N_S = 4$ and $N_L = 4, 8, 12, 16, 24, 32$, and 40, also show that set A gives the most reliable results. This may be contrasted with a calculation by Leichtberg *et al.* (1976*c*) for identical spheres having a relative velocity. They found that angles closer to the symmetry axis gave better results when the spheres were almost touching.

For touching spheres with relative volume of 10^3, table 2 gives the value of λ_S for combinations of N_S and N_L values using set A angles. The exact value is $\lambda = 0{\cdot}036370$. Two conclusions can be reached: (*a*) λ_S converges to the exact value as more multipoles are included, and (*b*) N_S is relatively unimportant if $N_S \geqslant 4$. Since larger values of N_S

N_S	N_L	A	B	C	G
2	2	0·66152	—	—	0·66152
4	4	0·64405	0·64770	0·64757	0·64411
8	8	0·64514	0·64568	0·64515	0·64487
12	12	0·64516	0·64514	0·64514	0·64514
4	8	0·64109	0·66572	0·69029	
		0·64842	0·62552	0·60284	
4	12	0·64034	0·70646	0·69405	
		0·64931	0·58760	0·59927	
4	24	0·64065	0·68991	0·68459	
		0·64896	0·60320	0·60818	
4	40	0·64065	0·68822	0·68474	
		0·64896	0·60479	0·60804	

TABLE 1. Drag coefficients for touching identical spheres using different collocation points. The exact value is 0·645141.

	N_S			
N_L	2	4	6	8
2	1·2946	1·7515	1·7577	1·7578
4	1·5034	2·0553	2·0626	2·0626
8	1·8598	2·6436	2·6520	2·6520
12	2·0044	3·0827	3·0886	3·0880
24	2·0774	3·6405	3·6270	3·6172
32	2·0580	3·7863	3·8207	3·7978

TABLE 2. Drag coefficient, $\lambda_S \times 10^2$, for small sphere following large sphere with relative volume of 10^3. Set A angles were used.

and N_L increase the chance of ill-conditioning in inverting the **M** matrix, we take $N_S = 4$ hereafter.

To see the effect of bunching the collocation points on the large particle surfaces near the point of contact, every second point on the surface away from the contact point was moved to the surface near the contact point. They were distributed at equal arc lengths but at an arc length away from the symmetry axis and an arc length away from the set A point closest to the axis. This set is called set D. Set E has points at 89° and 91° with $\frac{1}{4}$ the remaining points uniformly distributed on the surface away from the small particle and $\frac{3}{4}$ of the remaining points uniformly distributed on the surface of the large particle near the small particle. The point closest to the symmetry axis was always one arc from the axis. The results are shown in figure 3 along with the set A results. The values of λ increased with N_L more rapidly and for set D were close to the exact value of $N_L = 9$, 10 and 11. Similar values using set A required $N_L \gtrsim 20$. However sets D and E have wild fluctuations for $N_L \gtrsim 12$ and 15 respectively. This is very dramatic in the values of λ_L, the drag coefficient for the large particle. For set D we have $\lambda_L = 1{\cdot}007$, 0·9870, 0·9352, 3·591, 6·80 and 2·31 for $N_L = 7$, 9, 10, 11, 12 and 13 respectively. For set E we have $\lambda_L = 1{\cdot}016$, 0·8759, 1·001, 0·9563, 1·293 and $-1{\cdot}681$ for N_L equal to 11 through 16 respectively. Negative values also occur for set D at larger N_L values. For set A the value of λ_L varies from 0·9981 at $N_L = 5$ to 0·9964 for

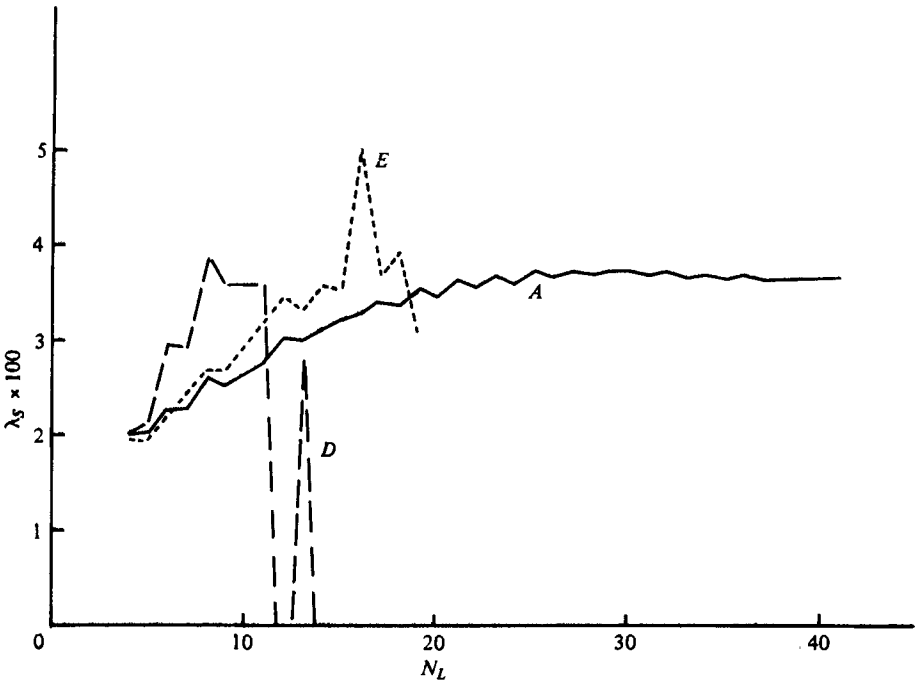

FIGURE 3. Drag coefficient $\times 10^2$ of a sphere touching a sphere of relative volume 10^3 as a function of the number of multipoles on the large particle using A, D, and E sets of angles.

$N_L = 23$. For $23 \leqslant N_L \leqslant 41$ we find $\lambda_L = 0{\cdot}9964$. To avoid these fluctuations in values as N_L is varied we have used points placed symmetrically about $\eta = \frac{1}{2}\pi$ in our subsequent calculations.

Other calculations for spheres with various relative volumes indicate that N_L should be roughly $4 \times V^{\frac{1}{3}}$ which is proportional to the ratio of the radii of the particles. As pointed out by a referee, this can be understood because 'the scale length of the disturbance reflected on the rearward portion of the leading sphere determines the number of boundary points and the characteristic wavelength of the Gegenbauer functions required. The disturbance created by the trailing spheroid decays as r^{-1} and this fixes the characteristic length for the interactive disturbance for the leading spheroid'. A more formal, though still not rigorous, justification is presented in appendix A.

(*c*) Results presented to this point indicate that we should use $N_S = 4$ and set A angles with points symmetrically placed about $\eta = \frac{1}{2}\pi$. We now investigate the number of multipoles required for the large particle, N_L, for relative volumes of 10, 10^2, and 10^3 for $\kappa_L = b_L/a_L = 0{\cdot}1$ and 10. For non-spherical particles set A points could be taken (*a*) as being separated by equal distances along the arc or (*b*) as being at points separated by equal intervals in the angle η. *A priori*, option (*a*) is attractive because it, in some sense, gives equal arc lengths equal weight. This argument is independent of the basic set of functions used in the expansion of ψ. Using option (*a*) we have calculated values for the drag coefficient for a small sphere in contact with the large particle as a function of N_L. The results are shown in figure 4, curves (*a*) to (*f*).

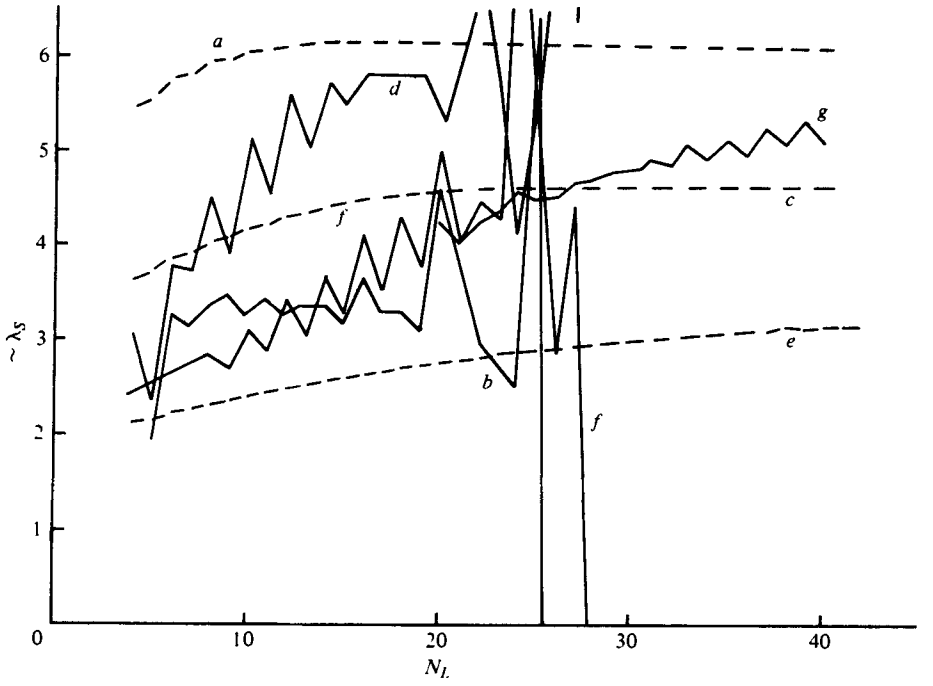

FIGURE 4. Drag coefficient for sphere touching a spheroid. For relative volume 10: (*a*) – – –, $10\lambda_S$ for $\kappa_L = 0{\cdot}1$; (*b*) ——, $10^2\lambda_S$ for $\kappa_L = 10$. For relative volume 10^2: (*c*) – – –, $10\lambda_S$ for $\kappa_L = 0{\cdot}1$; (*d*) ——, $10^3\lambda_S$ for $\kappa_L = 10$. For relative volume 10^3; (*e*) – – –, $10\lambda_s$ for $\kappa_L = 0{\cdot}1$; (*f*) ——, $5\times10^3\lambda_s$ for $\kappa_L = 10$; (*g*) $5\times10^3\lambda_S$ for $\kappa_L = 10$. For curves (*a*)–(*f*) the boundary conditions were applied at points separated by equal arc lengths. For curve (*g*) the angle η was divided into equal intervals.

For $\kappa_L = 0{\cdot}1$ the curves are smooth and appear to be approaching a value asymptotically. For $\kappa_L = 10$, however, there is a numerical instability for large N_L values. For relative volumes of 10 and 100 there is a plateau for $6 \leqslant N_L \leqslant 19$ and $16 \leqslant N_L \leqslant 19$ which we take as indicating the value of λ_S. This is, of course, uncertain. For relative volume of 1000 even an estimate is impossible. At the referee's suggestion which was based on an argument presented by Gluckman *et al.* (1971), we calculated the drag for $V = 10^3$ using option (*b*), i.e. equal η intervals. The results are shown in figure 4, curve (*g*). The fluctuations are significantly reduced for large values of N_L. Where the fluctuations are not large the two options agree. In retrospect option (*b*) is to be preferred.

As a partial check on these results, we calculated an approximate drag coefficient using the technique introduced by Goren & O'Neill (1971). They calculated the drag on a small sphere near a large sphere by first expanding the stream function assuming that the small sphere was not present. Expanding the stream function for the isolated L spheroid (oblate, prolate or sphere) moving at a velocity U, we obtain for r and $(x-a_L)$ small

$$\psi^* = -\tfrac{1}{2}A_0 r^2(x-a_L)^2, \tag{3.1}$$

where

$$A_0 = \tfrac{1}{3}(U/U_{tL})(a_L^2/b_L^2)(\rho_0-\rho)g/\mu. \tag{3.2}$$

This agrees with Goren and O'Neill for spheres, i.e. $b_L = a_L$. Using the Goren and O'Neill expression for the drag force on the small sphere in terms of A_0, we find an approximate value of

$$\lambda_{SA} = h^2\bar{f}_0(h/a_S)(\rho_0-\rho)g(3\kappa_L^2 U_{tL}\mu)^{-1}, \tag{3.3}$$

	Relative volume			
	1	10	10^2	10^3
$\kappa_L = 0{\cdot}1$	0·747	0·615	0·465	0·35
	595	128	27·6	5·95
$\kappa_L = 1{\cdot}0$	0·641	0·318	0·123	0·036
	4·85	1·04	0·225	0·0485
$\kappa_L = 10$	0·160	0·033	0·0058	—
	0·0890	0·0192	0·00413	0·000890

TABLE 3. Drag coefficient, λ_S, for particle touching L particle. Upper value is by collocation. Lower value is λ_{SA}.

where h is the distance of the centre of the small sphere from the surface of the spheroid. They give a table of values for $\bar{f}_0(h/a_S)$. In their derivation Goren & O'Neill treat the surface of the large particle as a planar surface. Thus we expect that λ_{SA} will be most accurate for large relative volumes (V_L/V_S). Also it should be more accurate for large oblate particles than for large prolate particles. This is verified by table 3 which presents the values of λ from the collocation calculation (upper value) and from equation (3.3) for several volumes and aspect ratios. These are for the small sphere in contact with the spheroid so $h = a_S$ and $\bar{f}_0(1) = 3{\cdot}2295$. Even for $V = 10^4$ and $\kappa_L = 1$, equation (3.3) gives a value 15 % larger than the exact value.

4. Numerical results for particle velocities

We now calculate the velocities of two particles acted upon by an external force such as gravity. The particles are assumed to interact with each other only through the fluid flow. Previous calculations were for spheres of different sizes by Wacholder & Sather (1974) and for identical prolate or oblate spheroids by Gluckman *et al.* (1971).

(*a*) We have checked our computer code by duplicating the results of Gluckman *et al.* for identical particles with $\kappa = 0{\cdot}2$, $0{\cdot}5$, $1{\cdot}0$, 2 and 5 with separations of their surfaces of zero and $14a$. A further consistency check was made for identical particles. The value of λ from § 3 and the value of U from this section must, because the particles travel at the same speed, satisfy

$$\lambda U = V(\rho_0 - \rho)g/(6\pi\mu b). \tag{4.1}$$

This equation does *not* hold for nonidentical particles. Our results were also checked with those of Wacholder and Sather for spheres of relative volume of 125.

(*b*) In general the relative motion of two spheres may be obtained by solving

$$dl/dt = U_S - U_L, \tag{4.2}$$

where U_S satisfies (Leichtberg *et al.* 1976*c*)

$$V_S\rho_0\frac{dU_S}{dt} = V_S\rho_0 g - V_S\rho g - 6\pi\mu U_S a\lambda_S - \tfrac{1}{2}V_S\rho\frac{dU_S}{dt} - 6a_S^2(\pi\mu\rho)^{\frac{1}{2}}\int_0^t \frac{dU_S}{d\tau}\frac{d\tau}{(t-\tau)^{\frac{1}{2}}} \tag{4.3}$$

and U_L satisfies a similar equation. The names given to the terms on the right-hand side of this equation are gravitational force, buoyancy force, Stokes drag, virtual mass

force, and the Basset force. Leichtberg *et al.* (1976*c*) have solved similar equations for three identical spheres for small Reynolds number flow. The Reynolds number is defined as $Re_\infty = 2aU_t\rho/\mu$, where U_t is the terminal velocity of an isolated particle. For times up to $180a/U_t$ they found that the inertial terms ($\sim dU_S/dt$) could be dropped with about 1 % error. For short times (up to about $50a/U_t$) the Basset term could also be dropped with less than about 10 % error. They also argued that the values of λ obtained in a steady-state calculation may be used.

The calculation of the velocities, U_S and U_L, as outlined in § 2 thus holds for short times, and one could calculate the separation $l(t)$ from the implicit equation

$$t - t_a = \int_{l_a}^{l} dl\,(U_S - U_L)^{-1}, \tag{4.4}$$

where l_a is the separation at time t_a.

(*c*) Before presenting the computer calculations we present analytic results which are valid for large separations. Happel & Brenner (1973) have discussed results obtained by Brenner (1964) for two widely separated particles. For two nonidentical spheroids aligned with a principal axis along the line of centres and with motion along the line of centres, using their results it is easy to show that

$$U_S = U_{St} + (\rho_0 - \rho)\,g a_L b_L^2 (3\mu l)^{-1} + O(l^{-3}), \tag{4.5}$$

where U_{St} is the terminal velocity of an isolated S particle. The expression for U_L may be obtained from this by interchange of S and L subscripts. The terminal velocity is

$$U_t = ab^2(\rho_0 - \rho)\,g(3\mu c)^{-1}\{\tfrac{1}{4}(p_0^2+1)\ln[(p_0+1)/(p_0-1)] - \tfrac{1}{2}p_0\} \tag{4.6a}$$

for a prolate spheroid and

$$U_t = ab^2(\rho_0 - \rho)\,g(3\mu c)^{-1}\{\tfrac{1}{2}(1-p_0^2)\,ctn^{-1}p_0 + \tfrac{1}{2}p_0\} \tag{4.6b}$$

for an oblate spheroid. For both cases $p_0 = a/c$. For a sphere we have

$$U_t = 2a^2(\rho_0 - \rho)\,g(9\mu)^{-1}. \tag{4.6c}$$

(*d*) We have calculated the velocities of two particles at various separations. The particles are uniform and have the same density. In figures 5–10 we present

$$(U_S - U_{St})/(U_{Lt} - U_{St}) \quad \text{and} \quad (U_L - U_S)/(U_{Lt} - U_{St})$$

as a function of $l/l_0 \geqslant 1$, where l is the separation of their centres and $l_0 = a_L + a_S$. For large separations the particles approach their terminal velocity, so these two quantities approach zero and one respectively. For particles in contact $U_L = U_S$, and, if the L particle is much larger than the S particle, then these quantities approach one and zero respectively. We have also plotted the expressions obtained by using the approximate values of U_S and U_L from the previous section. From the figures it is seen that these approximate forms are best for $\kappa < 1$ and for large relative volumes.

These calculations use collocation points separated by equal distances (defined as an arc length) along the particle surface with the topmost points at $\eta = 89°$ and $91°$. The lowest points are at one arc length away from the axis of symmetry. There are four points on the S particle. The number on the L particle, N_L, varied with both the relative volume of the particles and their separation. The values are given in table 4. For $l/l_0 \geqslant 1{\cdot}2$ the values of N_L gave results for $U_L - U_S$ which agreed to a fraction of a

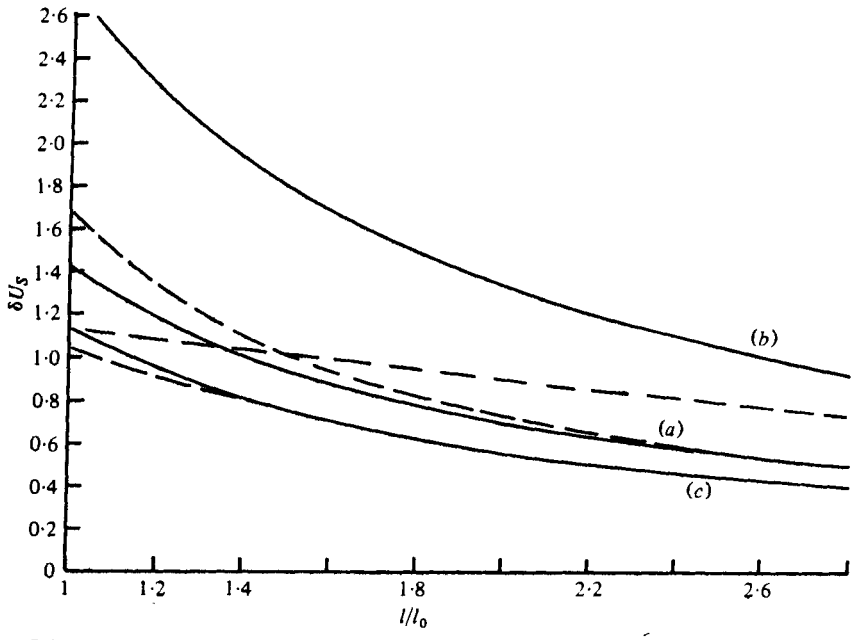

FIGURE 5. Velocity of S particles as a function of separation where $\delta U_S \equiv (U_S - U_{St})/(U_{Lt} - U_{St})$. $l/l_0 = 1$ for touching particles. $V = 1$. (κ_S, κ_L) are (0·1, 1) for (*a*), (10, 1) for (*b*), and (10, 0·1) for (*c*). Broken lines from collocation. Solid lines from asymptotic expressions.

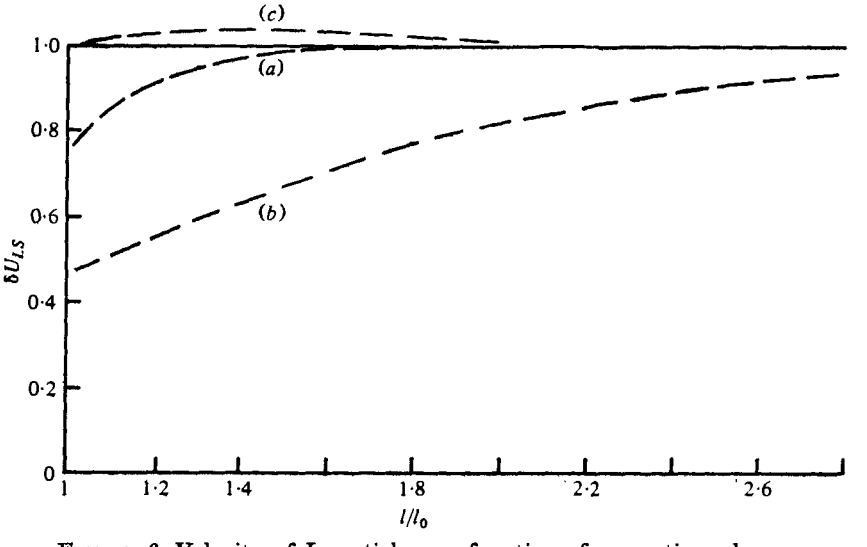

FIGURE 6. Velocity of L particle as a function of separation where $\delta U_{LS} \equiv (U_L - U_S)/(U_{Lt} - U_{St})$. $V = 1$.

per cent. For $l/l_0 < 1{\cdot}2$ larger N_L were used. The percentage change in $U_L - U_S$ indicates the accuracy of the result. It is possible that even fewer points would give accurate results. The large percentage change for $V = 10^3$, $\kappa_S = 10$ and $\kappa_L = 1$ is because $U_L - U_S$ is very close to zero at $l/l_0 = 1{\cdot}02$. Calculations of $U_L - U_S$ for two spheres of relative volumes of 125 and 1000 were compared with values obtained using equation (3.2) of

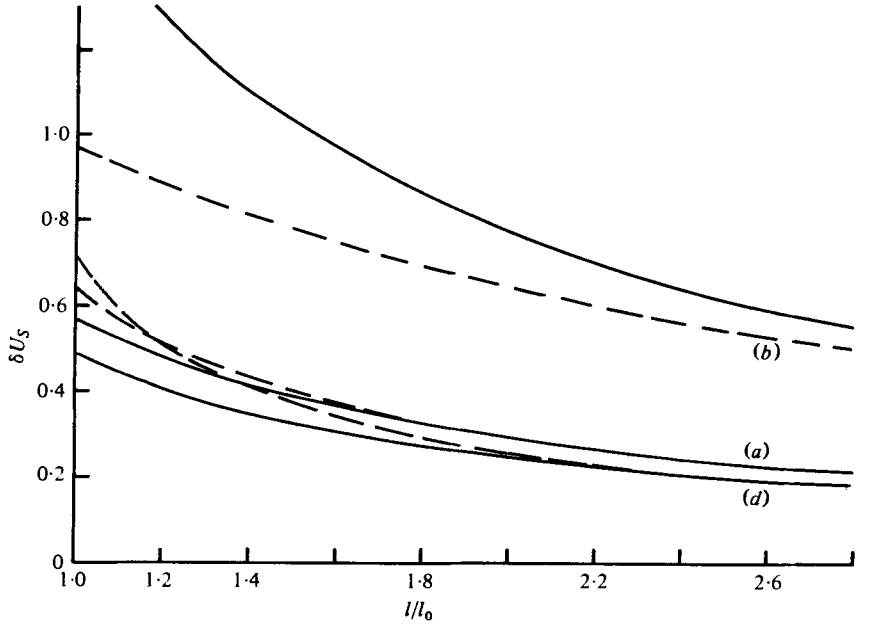

FIGURE 7. $(U_S - U_{St})/(U_{Lt} - U_{St})$ for $V = 10$.
$\kappa_S = 1$ and $\kappa_L = 0{\cdot}1$ for (*d*) curves.

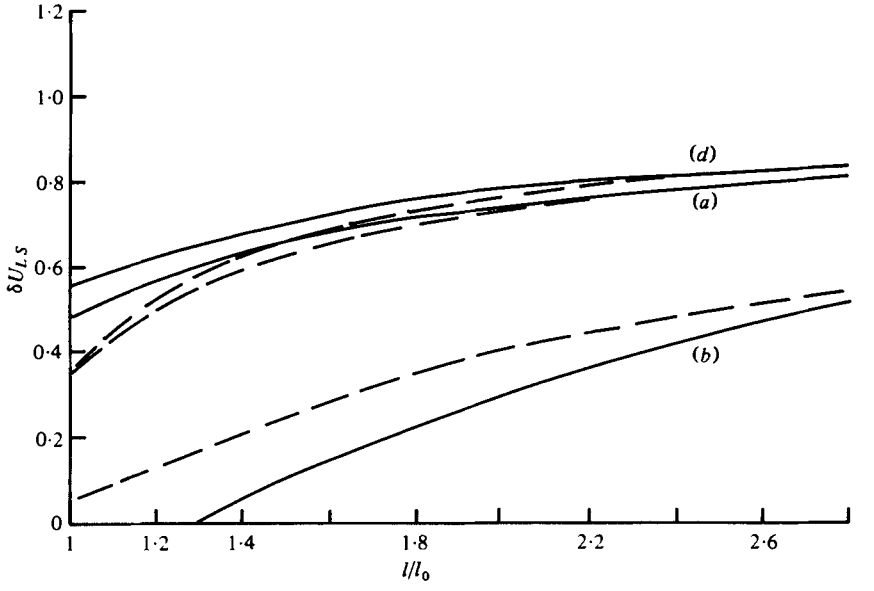

FIGURE 8. $(U_L - U_S)/(U_{Lt} - U_{St})$ for $V = 10$.

Wacholder and Sather for nearly touching spheres. For $V = 125$ the collocation results for $N_L = 30$ were larger by factors of 2·02, 1·28 and 1·04 for separations of $l/l_0 = 1{\cdot}01$, 1·02 and 1·03 respectively. For $V = 10^3$ the factors are 1·95, 1·27 and 1·07. Thus the difference of the velocities of nonidentical spheres at very small separations is not given accurately by the collocation technique. This result was previously discussed by

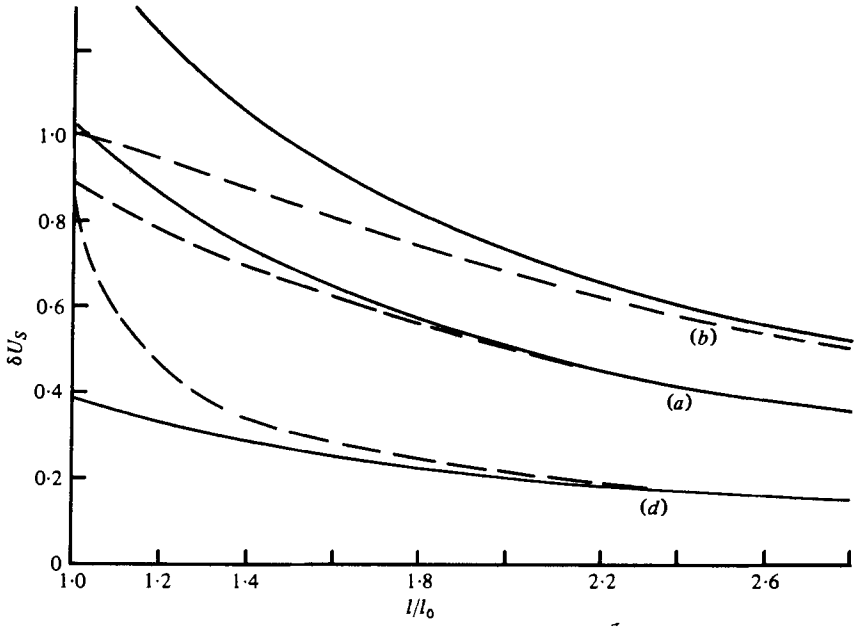

FIGURE 9. $(U_S - U_{St})/(U_{Lt} - U_{St})$ for $V = 1000$.

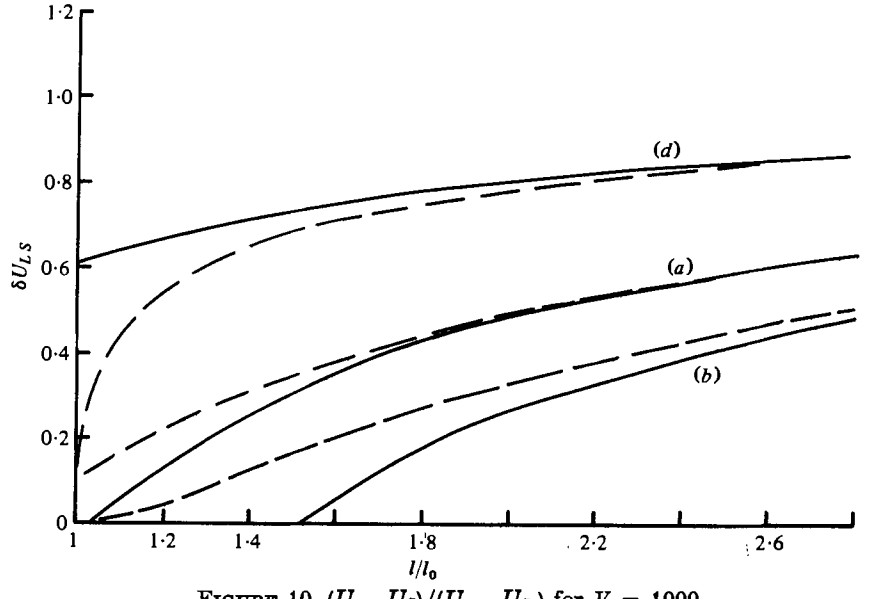

FIGURE 10. $(U_L - U_S)/(U_{Lt} - U_{St})$ for $V = 1000$.

Leichtberg *et al.* (1976*c*) for identical spheres. However, the percentage error in the individual velocities is quite small.

Figures 5–10 show that the velocities calculated to first order in l_0/l give quite good results for U_S and $U_L - U_S$ for $l \gtrsim 2l_0$. Results for prolate particles are more accurate than oblate particles.

V	κ_S	κ_L	$N_L^>$	$N_L^<$	$\Delta_{1\cdot02}$	$\Delta_{1\cdot1}$	$(U_L/U_{Lt})_{1\cdot0}$
1	0·1	1	4, 6	4, 6, 8, 12, 16	1 %	0·5 %	1·226
	10	1	—	—	0·1	0	1·278
	10	0·1	—	—	5	3·0	1·350
10	1	0·1	8, 10	8, 10, 12, 16, 20	2·0	0·2	1·044
	0·1	1	—	—	0·6	0·1	1·011
	10	1	—	—	11	2	1·016
10^3	1	0·1	16, 18	16, 18, 22, 26, 30	1	0	1·000
	0·1	1	—	—	1	0·2	0·9990
	10	1	—	—	300	11	1·001

TABLE 4. $N_L^>$, the number of points on the L particle for $l/l_0 \geqslant 1{\cdot}2$ and $N_L^<$ for l/l_0 less than 1·2. Δ, the percentage change in $(U_L - U_S)$ as N_L goes from its smallest value to its largest value for $l/l_0 = 1{\cdot}02$ and 1·1. The ratio U_L/U_{Lt} at $l/l_0 = 1{\cdot}02$.

Computations were performed on a CDC 6400 and CYBER 172 with nominal single precision of 16 digits. IMSL (International Mathematical and Statistical Libraries) subroutine LEQT2F was used to solve the matrix equations. This uses the Crout algorithm for Gaussian elimination with equilibration, partial pivoting, and iterative improvement as required.

5. Conclusions

The collocation technique of Gluckman *et al.* can be used to calculate the drag forces and axisymmetric motion of two spheroidal particles of different sizes and shapes. We have investigated the accuracy of these results as a function of (*a*) the number of collocation points, (*b*) the placement of the collocation points, (*c*) the shapes of the particles, (*d*) the relative volumes of the particles and (*e*) the separation of the particles. General results and conclusions include: (i) For large relative volumes ($V \sim 10^3$) and particles in contact the number of collocation points should be 4 on the small particle and approximately 40 on the large particle ($\sim 4V^{\frac{1}{3}}$). (ii) The points should correspond to equal angle, η, increments with points at $\eta = 89°$ and 91° except perhaps for the most nonspherical (i.e. $\kappa < 0{\cdot}1$ or $\kappa > 10$). (iii) Results for prolate spheroids converge, as a function of N_L, slowly but uniformly. Results for oblate spheroids may have wild fluctuations. (iv) The number of points required drops significantly (by factor of ~ 4) for separations of the centres of the particles on the order of twice the minimum separation. (v) For these separations the expansions to first order in l^{-1} from reflexion theory give more accurate results for prolate spheroids than for oblate spheroids. (vi) Reflexion theory improves as the relative volume increases. (vii) The technique of Goren & O'Neill (1971) for the drag on a small sphere near a large sphere was generalized to include a small sphere near a large spheroid. These approximate expressions are better for oblate spheroids than for prolate spheroids. (viii) The velocities of two different particles is given quite accurately ($\sim$ fraction of a per cent) by the collocation technique, but the difference in the velocities is probably in error by over 100 % for $l/l_0 \lesssim 1{\cdot}02$ and relative volume of 10^3. Three numerical improvements were introduced: (ix) A renormalization of the matrices reduced a possible 70 orders of magnitude difference in elements to a more manageable 4 orders of magnitude. (x) In some cases

more accurate results for the Gegenbauer functions may be obtained more quickly using the recursion relation downward rather than upward as has been done in previous calculations. This is especially important when many multipoles are included for large relative volumes. (xi) For oblate spheroids Gegenbauer functions of complex arguments are required. We have given a scheme for calculating these using only real quantities. Items (x) and (xi) allow us to use single-precision, real arithmetic on the computer rather than double-precision complex arithmetic as has been done in the past.

In view of (*a*) the number of choices to be made in a calculation (numbers of multipoles for each particle, the locations of the collocation points) and (*b*) the dependence of these upon the relative volumes, the particle shapes, and separation, it is recommended that the results given above be used as guides and not as rigid rules.

This work was supported by the Office of Naval Research through contracts N00014-67-A-0299-0020 and N00014-76-C-0250.

Appendix A

For two touching spheres of radii R_L and R_S and $R_L \gg R_S$, the stream function may be taken as

$$\psi = \psi_a + \psi_L + \psi_S, \tag{A 1}$$

where

$$\psi_a = U[1 - \tfrac{3}{2}(R_L/r_L) + \tfrac{1}{2}(R_L^3/r_L^3)]\, r_L^2 I_2(\cos\theta_L),$$

$$\psi_L = \sum_{n=2}^{\infty} (D_n/r_L^{n-3} + B_n/r_L^{n-1})\, I_n(\cos\theta_L)$$

and

$$\psi_S = \sum_{n=2}^{\infty} (d_n/r_S^{n-3} + b_n/r_S^{n-1})\, I_n(\cos\theta_S),$$

with r_L, θ_L and r_S, θ_S as the spherical co-ordinates with the origin at the centre of the large and small sphere respectively. ψ_a is the stream function for an isolated sphere of radius R_L. In general, to solve the problem completely, all the unknown constants (D_n, B_n, d_n, and b_n) must be retained to satisfy the no-slip boundary condition for all the points on the surface of two spheres. It will be demonstrated that d_2 depends significantly on $D_2, B_2, \ldots, D_n, B_n$, where n is approximately R_L/R_S. Note that d_2 is proportional to the drag force on the small sphere. For this, choose the approximate form:†

$$\psi_L = \sum_{n=2}^{\infty} (D_n/r_L^{n-3})\, I_n(\cos\theta_L) \quad \text{and} \quad \psi_S = d_2 r_S I_2(\cos\theta_S). \tag{A 2}$$

One boundary condition can be written as $\psi = 0$. On the surface of the large sphere, multiply ψ by $(I_n(\cos\theta_L)/(1-\cos^2\theta_L))$ and integrate with respect to $\cos\theta_L$ from $\cos\theta_L = -1$ to $+1$ and set $r_L = R_L$ to obtain

$$D_n = \frac{n(n-1)}{2(2n-1)(2n+1)} (R_L^{2n-3}/d^{n+1})\, ((2n+1)\, d^2 - (2n-1)\, R_L^2)\, d_2, \tag{A 3}$$

where $d = R_L + R_S$.

† Including b_2 and B_n ($n \geqslant 2$) in (A 2) and satisfying $\partial\psi/\partial r = 0$ in addition to $\psi = 0$ on the boundary makes the mathematics more complicated but the conclusion is the same.

Similarly, since $\psi = 0$ on all the points on the surface of the small sphere, multiply ψ by $(I_2(\cos\theta_S)/(1-\cos^2\theta_S)) = \frac{1}{2}$ and do the integration with respect to $\cos\theta_S$ and make the following approximation:

$$I_n(\cos\theta_L) \approx I_2(\cos\theta_L) = r_S^2 I_2(\cos\theta_S))/r_L^2, \tag{A 4}$$

and $r_L \approx d$ to obtain

$$\sum_{n=2}^{\infty} D_n(R_S/d^{n-1}) + d_2 = -\tfrac{9}{5}UR_S^3/R_L^2. \tag{A 5}$$

Substituting (A 3) into (A 5), and making the approximation:

$$(R_L/d)^n = (R_L/(R_L+R_S))^n \approx (1-R_S/R_L)^n \approx \exp(-nR_S/R_L) \tag{A 6}$$

gives the following for the left-hand side of (A 5):

$$d_2\left[\sum_{n=2}^{\infty}(R_S/R_L)\frac{n(n-1)}{(2n-1)(2n+1)}\exp(-2nR_S/R_L)\right]+d_2.$$

Solving for d_2 gives

$$d_2 \approx -\tfrac{9}{5}UR_S^3R_L^{-2}\left\{1+R_SR_L^{-1}\sum_{n=2}^{\infty}\frac{n(n-1)}{(2n-1)(2n+1)}\exp(-2nR_S/R_L)\right\}^{-1}. \tag{A 7}$$

Including more D_n and B_n is equivalent to including more terms in the summation in (A 7). Terms in this summation are of order unity for $n < R_L/R_S$ and thus on the order of R_L/R_S terms are required and R_L/R_S multipoles are required.

REFERENCES

Bowen, B. D. & Masliyah, J. H. 1973 *Can. J. Chem. Engng* **51**, 8.

Brenner, H. 1964 *J. Fluid Mech.* **18**, 144.

Cooley, M. D. A. & O'Neill, N. E. 1969 *Proc. Camb. Phil. Soc.* **66**, 407.

Ganatos, P., Pfeffer, R. & Weinbaum, S. 1978 *J. Fluid Mech.* **84**, 79.

Gautschi, W. 1967 *SIAM Rev.* **9**, 24.

Gluckman, M. J., Pfeffer, R. & Weinbaum, S. 1971 *J. Fluid Mech.* **50**, 705.

Gluckman, M. J., Weinbaum, S. & Pfeffer, R. 1972 *J. Fluid Mech.* **55**, 677.

Goren, S. L. 1970 *J. Fluid Mech.* **41**, 619.

Goren, S. L., & O'Neill, M. E. 1971 *Chem. Engng Sci.* **26**, 325.

Happel, J. & Brenner, H. 1973 *Low Reynolds Number Hydrodynamics.* Leyden: Noordoff.

Lamb, H. 1945 *Hydrodynamics.* New York: Dover.

Leichtberg, S., Pfeffer, R. & Weinbaum, S. 1976*a* *Int. J. Multiphase Flow* **3**, 147.

Leichtberg, S., Weinbaum, S. & Pfeffer, R. 1976*b* *Biorheology* **13**, 165.

Leichtberg, S., Weinbaum, S., Pfeffer, R. & Gluckman, M. J. 1976*c* *Phil. Trans. Roy. Soc.* A **282**, 585.

Liao, W. H. & Krueger, D. A. 1979 *J. Colloid Interface Sci.* **70**, 564.

O'Brien, V. 1968 *A.I.Ch.E. J.* **14**, 870.

Peterson, E. A. 1975 Concentration effects in ferrofluids. Ph.D. Thesis, Colorado State University.

Peterson, E. A. & Krueger, D. A. 1977 *J. Colloid Interface Sci.* **62**, 24.

PETERSON, E. A., KRUEGER, D. A., PERRY, M. & JONES, T. B. 1975 In *Concentration Effects in Ferrofluids* (ed. C. D. Graham, G. H. Lander, & J. J. Rhyne), AIP Conf. Proc. no. 24, p. 560. Amer. Phys. Int., New York.

STIMSON, M. & JEFFERY, O. B. 1926 *Proc. Roy. Soc.* A **111**, 110.

WACHOLDER, E. & SATHER, N. F. 1974 *J. Fluid Mech.* **65**, 417.

YOUNGREN, G. K. & ACRIVOS, A. 1975*a* *J. Fluid Mech.* **69**, 337. Corrigendum: 1976 *J. Fluid Mech.* **75**, 813.

YOUNGREN, G. K. & ACRIVOS, A. 1975*b* *J. Chem. Phys.* **63**, 3846.

YOUNGREN, G. K. & ACRIVOS, A. 1976 *J. Fluid Mech.* **76**, 433.